

4-2018

# Twinning Strains in Synfolding Calcite, Proterozoic Sinian System, China

John P. Craddock

*Macalester College*

Junlai Liu

*China University of Geoscience Beijing*

YuanYuan Zheng

*China University of Geoscience Beijing*

Follow this and additional works at: <https://digitalcommons.macalester.edu/geolfacpub>



Part of the [Geology Commons](#)

---

## Recommended Citation

Craddock, John P.; Liu, Junlai; and Zheng, YuanYuan, "Twinning Strains in Synfolding Calcite, Proterozoic Sinian System, China" (2018). *Faculty Publications*. 1.

<https://digitalcommons.macalester.edu/geolfacpub/1>

This Article is brought to you for free and open access by the Geology Department at DigitalCommons@Macalester College. It has been accepted for inclusion in Faculty Publications by an authorized administrator of DigitalCommons@Macalester College. For more information, please contact [scholarpub@macalester.edu](mailto:scholarpub@macalester.edu).

Short Note

# Twinning Strains in Synfolding Calcite, Proterozoic Sinian System, China

John P. Craddock <sup>1,\*</sup>, Junlai Liu <sup>2</sup> and Yuanyuan Zheng <sup>2</sup>

<sup>1</sup> Geology Department, Macalester College, St. Paul, MN 55105, USA

<sup>2</sup> State Key Laboratory of Geological Processes and Mineral Resources and Key Laboratory of Lithosphere Tectonics, China University of Geosciences, 29 Xueyuan Rd., Beijing 100083, China; jliu@cugb.edu.cn (J.L.); yyzh0309@126.com (Y.Z.)

\* Correspondence: craddock@macalester.edu

Received: 1 March 2018; Accepted: 6 April 2018; Published: 11 April 2018



**Abstract:** Synfolding calcite was precipitated between layers of Neoproterozoic sandy dolomite and striated parallel to the fold axis of an open anticline with a shallow plunge during folding. The fold had limb dips of 45° and plunged 20° to the south. The synfolding calcite had sub-horizontal grooves that trended parallel to the fold. Limb-hinge-limb calcite samples (3 samples;  $n = 100$  grains) preserved a layer-parallel shortening strain that trended at an acute (45°) angle to the trend of the fold axis and fold lineations. Extension axes were vertical and there was no strain overprint (low NEVs). Shortening strain magnitudes were −2.9% and the differential stress responsible for twinning was −38 MPa. The commonly observed structures were layer-parallel slip striations normal to the fold axis: sub-horizontal interlayer slip surfaces parallel to a fold axis (parallel to bedding strike) were unreported; as was a sub-horizontal shortening strain at an acute angle to the axis of a plunging fold.

**Keywords:** structural geology; folding dynamics; strain analysis

## 1. Introduction

Folds are common observations in most deformed regions and in rocks of low metamorphic grade, the folding mechanism is often accommodated by a layer-parallel slip on bedding planes normal to the fold axis (flexural-slip folding; [1,2]) often accompanied by the development of an axial planar cleavage. Numerous studies of folding dynamics have utilized the presence of intergranular deformation lamellae in quartz and/or calcite to understand fold genesis, whether within regional [2–21]. The dominant fabric preserved is a pre-folding, layer-parallel shortening (LPS) strain within the plane of fault transport (plane strain) with little or no synfolding strain overprint of the early LPS fabric, but with evidence of complex strain partitioning (e.g., [17]). Subsequent strain studies using synfolding calcite have reported a variety of anomalous results (Laramide Derby dome, Wyoming, [22]; Cape fold belt, [23]; Alpine folds in Crete, [24]). The fold described here had interlayered synfolding calcite layers (that crosscut and were continuous across beds in places) with horizontal striations parallel to the south-plunging fold axis suggesting that layer-parallel shortening, with the shortening axis normal to the fold axis, would *not* be the expected strain recorded by the twinned calcite in this fold. Our goal was to investigate the stress-strain history of this unique fold by presuming that the synfolding calcite layers precipitated, and the calcite twinned mechanically during folding, a process of interest to structural geologists.



## 2. Methods

### *Calcite Twin Analysis*

The calcite strain-gage technique (CSGT) of Groshong [25] allows the investigation of intraplate stresses as conserved by intracrystalline twinning of rock-forming calcite grains. Although the result is actually a strain tensor, a similar orientation of the stress tensor appears likely in the case of coaxial deformation [26,27]. The CSGT has been used to constrain strain tensor directions in veins [28], limestones [17,29–34], marble [35,36] and lamprophyres [37].

Below temperatures of ca. 200 °C, intracrystalline deformation of calcite results in the formation of e-twins. The formation of calcite e-twins requires a shear stress exceeding ca. 10 MPa [38–41]. Calcite offers three glide systems for e-twinning. From the U-stage measurements of width, frequency, and orientation of twins, and the crystallographic orientation of the host crystals, a strain tensor can be calculated using a least-squares technique [25]. In order to remove “noise” from the dataset, a refinement of the calculated strain tensor can be achieved by stripping 20% of the twins with the highest deviations [42]. This procedure has been used when the number of measured grains was large ( $n > 20$ ). In cases where the data appear to be inhomogeneous, the separation of incompatible twins (“(LPS)” = negative expected values) from compatible twins (“(POS)” = positive expected values) of the initial dataset allows the separate calculation of two or more least-squares deviatoric strain tensors. Thus, the CSGT can be used to obtain information on superimposed deformations [25,43] and differential stress magnitudes [44].

The validity of this stripping procedure has been demonstrated in experimental tests; the reliability depends on the overall complexity of deformation and the number of grains with twins [43,45]. The stripping procedure has been used in cases of high proportions of negative expected values (NEVs) and a high number of measured grains. An experimental re-evaluation of the CSGT has shown that measurements of about 50 grains on one thin-section, or 25 grains on two mutually perpendicular thin-sections, yielded the best results [42,46,47]. The chance to extract the records of more than two deformations from one dataset is limited when dealing with natural rocks [39]. Individual analyses of veins, matrix, or nodules allows the acquisition of several strain tensors without applying statistical data stripping. The complexity of rotational strains in fault zones has limited the application of this method to the efforts of Gray et al. [48]. Application of the CSGT requires the following assumptions to be valid: (1) low temperatures (dominance of Type I and Type II twins); (2) random c-axis orientations of calcite; (3) homogenous strain; (4) coaxial deformation; (5) volume constancy; (6) low porosity materials; and (7) low strain (<15%; [42]). If these conditions are not fully met, the underlying dataset of the calculated strain tensor can be biased, modified, or random. Strain tensors were calculated from calcite e-twin datasets using the software package of Evans and Groshong [46].

## 3. Results

### *3.1. Field Relations*

The Liaodong Peninsula, the east extension of the North China craton in NE China, is composed of two basic stratigraphic units separated by a curved detachment fault of the Liaonan metamorphic core complex (Figure 1). Neoproterozoic tonalites and supracrustal rocks, and Paleoproterozoic metasedimentary rocks form a crystalline basement of amphibolite grade in the lower plate of the Cretaceous core complex. Overlying the basement is a weakly metamorphosed Neoproterozoic to Carboniferous sedimentary cover and a Cretaceous marine section that was gently folded during exhumation of the core complex [49].

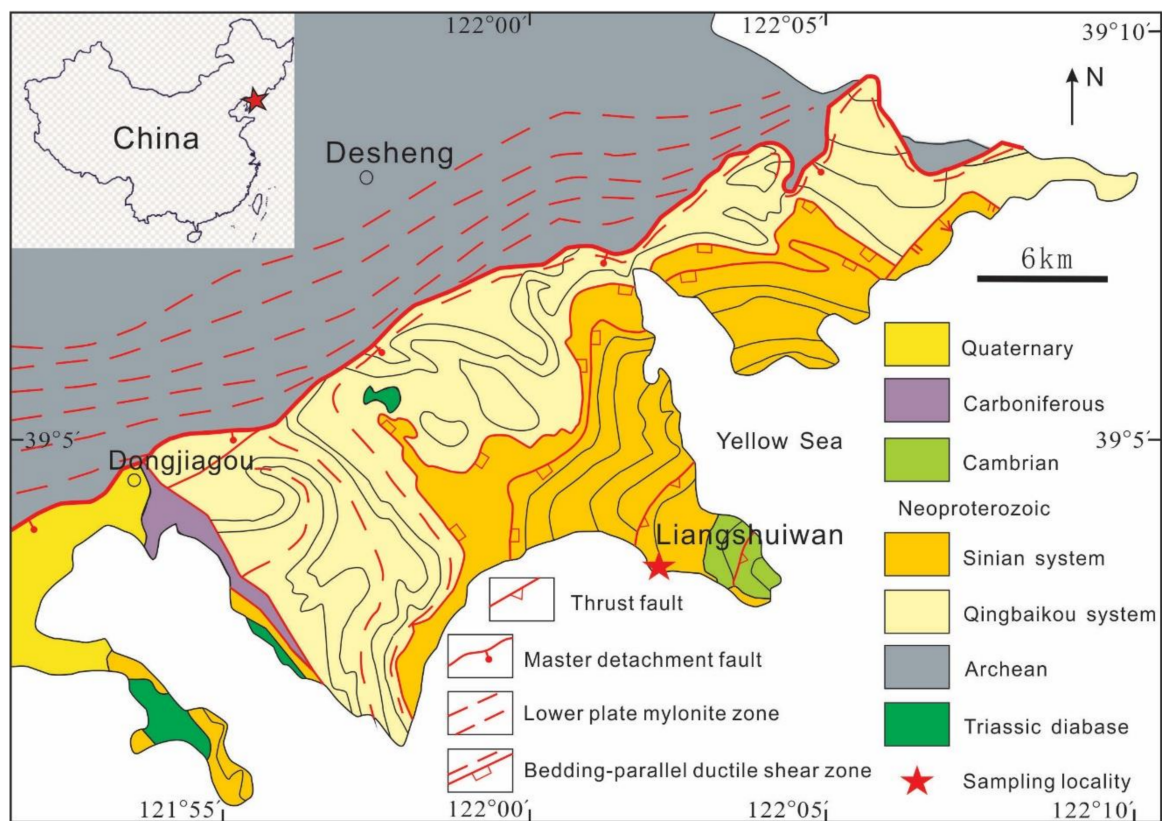


**Figure 1.** Location map of the field area and geology on the Liaonan Peninsula in Northeast China.

The Neoproterozoic Sinian System, from which the samples were taken, consists of a thick sequence of shallow marine sediment, i.e., sandstones, shales, limestones, or dolomitic limestones with stromatolitic layers (Figure 2). The Neoproterozoic section is unconformably overlain by a Cambrian–Carboniferous marine section, and the region was deformed in the Triassic by the amalgamation of the Yangtze and North China plates at ca. 220 Ma [50]. The Archean footwall gneisses of the Liaonan metamorphic core complex (trend: N 45° E) include a mylonite in fault contact with Cretaceous and older rocks; the mylonite includes folds (trend: N 45° E, vergence is ~N 45° W) and a lineation (N 45° W; upper plate translation to the NW) that are not consistent with a deformational correlation between the Cretaceous core complex formation and the N–S trending folds 20 km south hosted in the Sinian System in our study [49,51]. Calcite strain studies in the Liaonan core complex hanging wall Cretaceous limestones and veins preserve a shortening strain parallel to the axis of the core complex [52].

The field site is characterized by open anticline-syncline pairs, most of which plunge to the south (Figure 2A). Stromatolites are common and often overturned (Figure 2B). An axial planar cleavage is not present, but synfolding calcite layers are common between most of the bedding planes and these preserve horizontal striations (grooves) parallel to the fold axis, but are without fibrous kinematic steps. Calcite layers are bedding-parallel, but do crosscut bedding and connect across layering. The sample location was 39°04′29.00″ N, 122°01′44.36″ E.

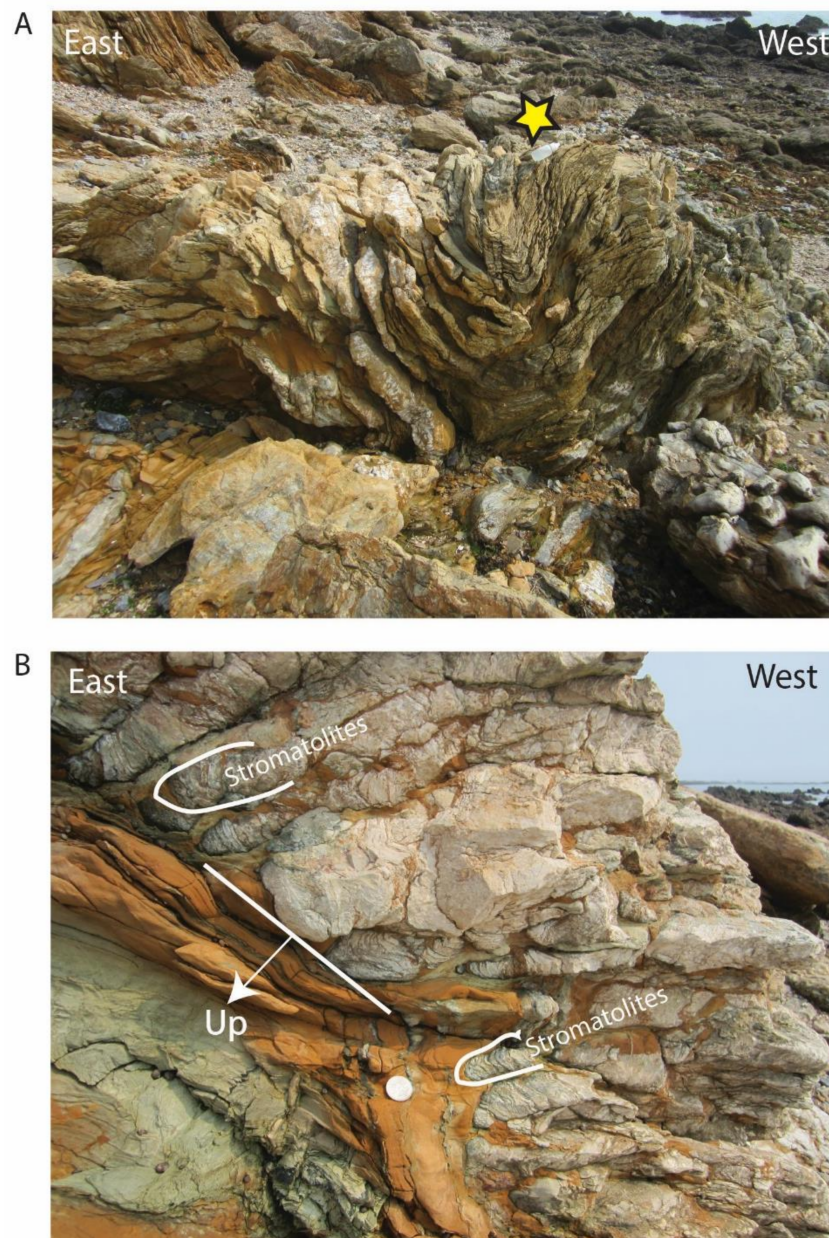


**Figure 2.** The minor fold with synfolding calcite and horizontal, grooved synfolding calcite (A; acid bottle by star for scale) is found along the shoreline in proximity to overturned Proterozoic stromatolites (B; coin for scale).

### 3.2. Synfolding Twinning in Calcite

Three samples were collected across the fold (Figures 2A and 3A) from inter-layered synfolding calcite. The calcite is sparry and most grains contain 1 twin set whereas the host sediment is a sandy, micritic dolostone without twins. Each sample recorded a sub-horizontal, layer-parallel shortening strain (NE–SW) at an acute angle to the fold axis and striations ( $L_1$ ) in the synfolding calcite (Figure 3, Table 1). Extension axes were vertical, the shortening strains average  $-2.9\%$  and were the result of a differential stress of  $-38.3$  MPa. Shortening axes intersected both the plane of the synfolding calcite and bedding so the fabric can be interpreted as vein and layer-parallel shortening (Table 1). Calcite optic axes ( $n = 100$ ) showed no preferred orientation (Figure 3B). Since there was no parallelism between these structures and the nearby Cretaceous metamorphic core complex, and since the twinned calcite had low NEVs (no twinning overprint), the fold in question was presumed to have formed



during the Triassic orogenesis with no younger overprint. Attempts to date the synfolding calcite failed due to low U levels (see [53]).

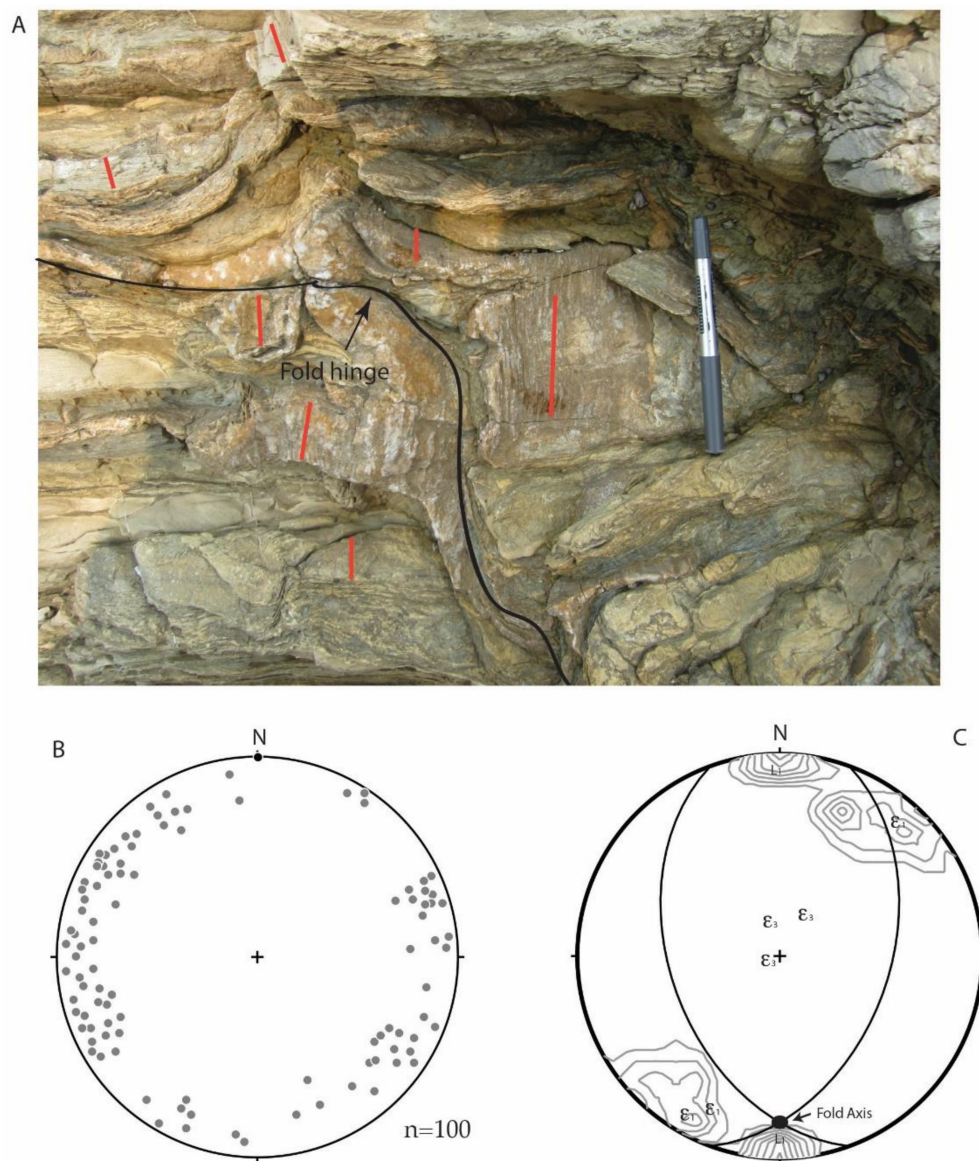


**Figure 3.** Oblique view down at the fold hinge showing the striated calcite parallel to the fold axis (A; pen for scale). Lower hemisphere projection of the combined optic axis data (B) and the limb-hinge-limb strain data (Table 1) where great circles are bedding planes for the fold that plunges 20° south (C). Fold axis-parallel lineations are contoured, as are Turner [26] compression axes. Shortening ( $\epsilon_1$ ) and extension ( $\epsilon_3$ ) strain axes were plotted for the three samples.

**Table 1.** Synfolding Calcite Twinning Data.

Sample	Rock Unit	Orientation	Grains (n=)	$\epsilon_1$	$\epsilon_2$	$\epsilon_3$	e1 (%)	NEV (%)	$\Delta\sigma$ (MPa)	Fabric Interp.
(Bedding)										(Vein)
Limb	Sinian System	N 25° E, 45° SE	34	46°, 4°	145°, 12°	278°, 82°	−1.8	11	−38.6	VPS, LPS
Hinge	Sinian System	N 90° E, 20° S	33	212°, 14°	303°, 28°	37°, 61°	−5.7	0	−38.3	VPS, LPS
Limb	Sinian System	N 25° W, 45° SW	33	214°, 7°	138°, 11°	3°, 72°	−1.2	6	−38.2	VPS, LPS
<i>n</i> = 100									Avg = −38.3	

Note: VPS = vein-parallel shortening; LPS = layer-parallel shortening.

#### 4. Discussion

Layer-parallel shortening was preserved by the mechanical twins in calcite precipitated along the bedding planes of the Proterozoic Sinian System sediments as these rocks were deformed in the Triassic. The tectonic transport direction was ~SW–NE and minor fold axes were at an acute angle to this margin. The shortening axes were sub-horizontal and oriented NE–SW at an acute angle to the N–S fold axis and the striations ( $L_1$ ) in the layers of calcite, or parallel to the Triassic tectonic margin. Both the observation of the horizontal, fold axis-parallel striations in the synfolding calcite, the resultant calcite twinning strain, and the tectonic orientation of both, were unusual for a minor fold that may have formed by buckling [12,54]. Spang and Groshong [17] reported the most comprehensive study of a minor fold where layer-parallel shortening was the early strain, followed by a complex interplay of fracturing, vein filling, pressure solution, and secondary twinning of calcite veins; the fold studied here only allowed for analysis of the synfolding calcite. High-grade metamorphic rocks often contain boudinage structures where metamorphic minerals are lineated parallel to the long axes (or normal to the boudin necks) of the boudins and fold axes (see [55]); the observation did not correlate well with our low-grade fold structure and there have been no syn-boudin strain studies reported.

The Derby dome is a thick-skinned Laramide structure formed in the foreland where the pre-folding LPS strain fabric can be used as a passive strain marker to interpret fold development. Orogenic LPS fabrics are known to occur at great distances into the craton of a continent [31,56,57] and different orogenic regions preserve unique LPS fabrics across North America [58,59] or within the individual thrust sheets of an orogenic belt [60,61]. The twinned calcite in the country rock of the Derby dome preserves this early (Sevier), E–W layer-parallel fabric strain and does not record any twinning strain overprint (low NEVs) as these sediments were folded into the dome structure. As the LPS fabric was rotated from an E–W orientation into parallelism with the Derby fold axis (N 30° W), the synorogenic calcite veins preserved a very complex stress-strain field that was not plane strain as the fold axis was overturned and offset by a NE-dipping thrust fault [22].

Strain studies of synfolding calcite have also been reported from Permian sediments at the northern end of the Gondwanide Cape fold belt [23]. In this setting, calcite and quartz was precipitated along the bedding planes during folding, and striations were observed parallel to the tectonic transport direction (N–S). The calcite was twinned and only undulatory extinction was observed in quartz. The twinning strain revealed an N–S layer-parallel shortening, but also a strain overprint preserving a flexural-slip rotation through this minor, upright syncline from SW to NE.

Alpine nappe structures are found throughout Crete including the Cretaceous Pindo limestones folded in the Pindos nappe [24,62]. A minor, upright anticline here preserves a layer-parallel shortening strain normal to the fold axis, the expected result. Calcite also fills an axial planar cleavage and is twinned: a sub-horizontal shortening strain is recorded parallel to the fold axis and the strike of the cleavage planes, a result somewhat similar to the fold result presented in this paper.

## 5. Conclusions

The dynamics of folding of the Proterozoic Sinian dolostone and synfolding, layer-parallel calcite suggests that horizontal tectonic stresses compressed the region in the Triassic and this minor fold shortened at  $\sim 45^\circ$  to the fold axis (parallel to the Triassic margin) and was accommodated by a layer-parallel slip parallel to the N-S fold axis as part of the larger, regional nappe formation. The dynamics of this minor fold could be classified as “passive” in that the extension axes ( $\epsilon_3$ ) were all vertical in the limb-hinge-limb samples and not everywhere in the bedding-normal as might be found in a buckle or flexural-slip fold. Without an absolute age for the synfolding calcite layers, the striations on the calcite layers and the twinning strains could be post-folding. The synfolding calcite was presumed to be Triassic and not younger, partly because there was no twinning strain overprint related to the nearby Cretaceous Liaonan metamorphic core complex and the Liaonan strain orientations are different and the penetrative deformation is limited to the core complex detachment [49].

**Acknowledgments:** The project was supported by the National Natural Science Foundation of China grants 90814006, 91214301 and 41430211 to LIU. Student field support by Ruoyu Zhang, Haonan Gan, Tingting Zhang, Hongke Li, Nikita Avdievitch, and Julia Carrizosa is greatly appreciated. Avdievitch was supported by a Wallace grant from Macalester College.

**Author Contributions:** John P. Craddock (field, strain measuring, writing), Junlai Liu (field and writing), and Yuanyuan Zheng (field and writing). The authors appreciate the constructive and helpful critiques by two anonymous reviewers.

**Conflicts of Interest:** We have no conflicts of interest to declare.

## References

1. Ramsay, J.G. *Folding and Fracturing in Rocks*; McGraw-Hill Publishers: New York, NY, USA, 1967; p. 568.
2. Chapple, W.M.; Spang, J.H. Significance of layer parallel slip during folding of layered sedimentary rocks. *Geol. Soc. Am.* **1974**, *85*, 1523–1534. [[CrossRef](#)]
3. Carter, N.L.; Friedman, M. Dynamic analysis of deformed quartz and calcite from the Dry Creek Ridge anticline, Montana. *Am. J. Sci.* **1965**, *262*, 747–785. [[CrossRef](#)]
4. Burger, R.; Hamill, M.N. Petrofabric stress analysis of the Dry Creek Ridge anticline, Montana. *Geol. Soc. Am. Bull.* **1976**, *87*, 555–566. [[CrossRef](#)]
5. Friedman, M.; Stearns, D.W. Relations between Stresses inferred from Calcite Twin Lamellae and Macrofractures, Teton Anticline, Montana. *Geol. Soc. Am. Bull.* **1971**, *82*, 3151–3162. [[CrossRef](#)]
6. Schmid, S.M.; Casey, M.; Starkey, J. The microfabric of calcite tectonites from the Helvetic Nappes (Swiss Alps). In *Thrust and Nappe Tectonics*; The Geological Society of London: London, UK, 1981; pp. 151–158.
7. Hennings, P. Petrofabric implications for cover rock adjustment in basement-cored anticline: Dry Fork Ridge, Bighorn Mtns, Wyoming. *Geol. Soc. Am. Abstr. Programs* **1986**, *18*, 635.
8. Hennings, P. Basement-Cover Relations of the Dry Fork Ridge Anticline Termination, Northeastern Bighorn Mountains, Wyoming and Montana. MSc Thesis, Texas A&M University, College Station, TX, USA, 1986.
9. Fisher, D.M.; Anastasio, D.J. Kinematic analysis of a large scale leading edge fold, Lost River Range, Idaho. *J. Struct. Geol.* **1994**, *16*, 337–354. [[CrossRef](#)]
10. Scott, W.H.; Hansen, E.; Twiss, R.J. Stress analysis of quartz deformation lamellae in a minor fold. *Am. J. Sci.* **1965**, *263*, 729–746. [[CrossRef](#)]
11. Spang, J.H. Numerical dynamic analysis of calcite twin lamellae in the Greenport Center syncline. *Am. J. Sci.* **1974**, *274*, 1044–1058. [[CrossRef](#)]
12. Groshong, R.H., Jr. Strain, fractures, and pressure solution in natural single-layer folds. *Bull. Geol. Soc. Am.* **1975**, *86*, 1363–1376. [[CrossRef](#)]
13. Mitra, G. Microscopic deformation mechanisms and flow laws in quartites within South Mountain anticline. *J. Geol.* **1978**, *86*, 129–152. [[CrossRef](#)]
14. Oertel, G. Strain in ductile rocks on the convex side of a folded competent bed. *Tectonophysics* **1980**, *66*, 15–34. [[CrossRef](#)]

15. Spang, J.H.; Simony, P.S.; Mitchell, W.J. Strain and folding mechanism in a similar style fold from the northern Selkirks of the Canadian Cordillera. *Tectonophysics* **1980**, *66*, 253–267. [[CrossRef](#)]
16. Spang, J.H.; Wolcott, T.L.; Serra, S. *Strain in the Ramp Regions of Two Minor Thrusts, Southern Canadian Rocky Mountains*, American Geophysical Union Monograph 24; American Geophysical Union: Washington, DC, USA, 1981; pp. 243–250.
17. Spang, J.H.; Groshong, R.H., Jr. Deformation mechanisms and strain history of a minor fold from the Appalachian Valley and Ridge Province. *Tectonophysics* **1981**, *72*, 323–342. [[CrossRef](#)]
18. Hudleston, P.J.; Holst, T.B. Strain analysis and fold shape in a limestone layer and implications for layer rheology. *Tectonophysics* **1984**, *106*, 321–347. [[CrossRef](#)]
19. Onasch, C.M. Petrofabric test of viscous folding theory. *Tectonophysics* **1984**, *106*, 141–153. [[CrossRef](#)]
20. Narahara, D.K. Wiltschko, Deformation in the hinge region of a chevron fold, Valley and Ridge Province, central Pennsylvania. *J. Struct. Geol.* **1986**, *8*, 157–168. [[CrossRef](#)]
21. Hudleston, P.J.; Tabor, J.R. Strain and fabric development in a buckled calcite vein and rheological implications. *Bull. Geol. Inst. Univ. Ups.* **1988**, *14*, 79–94.
22. Craddock, J.P.; Relle, M.K. Fold axis-parallel rotation within the Laramide Derby Dome fold, Wind River basin, WY. *J. Struct. Geol.* **2003**, *25*, 1959–1972. [[CrossRef](#)]
23. Craddock, J.P.; McKiernan, A.; DeWit, M. Calcite twin analysis in synorogenic calcite, Cape Fold Belt: Implications for fold rotation and cleavage formation. *J. Struct. Geol.* **2007**, *27*, 1100–1113. [[CrossRef](#)]
24. Craddock, J.P.; Klein, T.; Kowalczyk, G.; Zulauf, G. Calcite twinning strains in Alpine orogen flysch: Implications for thrust-nappe mechanics and the geodynamics of Crete. *Lithosphere* **2009**, *1*, 174–191. [[CrossRef](#)]
25. Groshong, R.H., Jr. Strain calculated from twinning in calcite. *Bull. Geol. Soc. Am.* **1972**, *83*, 2025–2038. [[CrossRef](#)]
26. Turner, F.J. Nature and dynamic interpretation of deformation lamellae in calcite of three marbles. *Am. J. Sci.* **1953**, *251*, 276–298. [[CrossRef](#)]
27. Turner, F.J. Compression and tension axes deduced from (0112) Twinning in Calcite. *J. Geophys. Res.* **1962**, *67*, 1660.
28. Kilsdonk, W.; Wiltschko, D.V. Deformation mechanisms in the southeastern ramp region of the Pine Mountain block, Tennessee. *Geol. Soc. Am. Bull.* **1988**, *100*, 644–653. [[CrossRef](#)]
29. Engelder, T. The nature of deformation within the outer limits of the central Appalachian foreland fold-and-thrust belt in New York state. *Tectonophysics* **1979**, *55*, 289–310. [[CrossRef](#)]
30. Wiltschko, D.V.; Medwedeff, D.A.; Millson, H.E. Distribution and mechanisms of strain within rocks on the northwest ramp of Pine Mountain block, southern Appalachian foreland: A field test of theory. *Geol. Soc. Am. Bull.* **1985**, *96*, 426–435. [[CrossRef](#)]
31. Craddock, J.P.; van der Pluijm, B.A. Late Paleozoic deformation of the cratonic carbonate cover of eastern North America. *Geology* **1989**, *17*, 416–419. [[CrossRef](#)]
32. Mosar, J. Internal deformation in the Prealpes Medianes, Switzerland. *Eclogae Geol. Helv.* **1989**, *82*, 765–793.
33. Ferrill, D.A. Calcite twin widths and intensities as metamorphic indicators in natural low-temperature deformation of limestone. *J. Struct. Geol.* **1991**, *13*, 675–677. [[CrossRef](#)]
34. Craddock, J.P.; Neilson, K.J.; Malone, D.H. Calcite twinning strain constraints on Heart Mountain detachment kinematics, Wyoming. *J. Struct. Geol.* **2000**, *22*, 983–991. [[CrossRef](#)]
35. Craddock, J.P.; Moshian, A.; Pearson, A.M. Kinematic analysis from twinned calcite strains in the marble mylonites of the central Grenville province, Canada. *Geol. Soc. Am. Abstr. Programs* **1991**, *15*, 236.
36. Craddock, J.P.; Pearson, A. Non-coaxial horizontal shortening strains preserved in amygdule calcite, DSDP Hole 433C, Suiko Seamount. *J. Struct. Geol.* **1994**, *16*, 719–724. [[CrossRef](#)]
37. Craddock, J.P.; Anziano, J.; Wirth, K.R.; Vervoort, J.D.; Singer, B.; Zhang, X. Structure, geochemistry and geochronology of a lamprophyre dike swarm, Archean Wawa terrane, Michigan, USA. *Precambrian Res.* **2007**, *157*, 50–70. [[CrossRef](#)]
38. Wenk, H.-R.; Takeshita, T.; Bechler, E.; Erskine, B.G.; Matthies, S. Pure Shear and Simple Shear Calcite Textures. Comparison of Experimental, Theoretical and Natural Data. *J. Struct. Geol.* **1987**, *9*, 731–745. [[CrossRef](#)]



39. Burkhard, M. Calcite twins, their geometry, appearance and significance as stress-strain markers and indicators of tectonic regime: A review. *J. Struct. Geol.* **1993**, *15*, 351–368. [\[CrossRef\]](#)
40. Lacombe, O.; Laurent, P. Determination of deviatoric stress tensors based on inversion of calcite twin data from experimentally deformed monophase samples: Preliminary results. *Tectonophysics* **1996**, *255*, 189–202. [\[CrossRef\]](#)
41. Ferrill, D.A. Critical re-evaluation of differential stress estimates from calcite twins in coarse-grained limestone. *Tectonophysics* **1998**, *285*, 77–86. [\[CrossRef\]](#)
42. Groshong, R.H., Jr.; Teufel, L.W.; Gasteiger, C.M. Precision and accuracy of the calcite strain-gage technique. *Bull. Geol. Soc. Am.* **1984**, *95*, 357–363. [\[CrossRef\]](#)
43. Groshong, R.H., Jr. Experimental test of least-squares strain calculations using twinned calcite. *Bull. Geol. Soc. Am.* **1974**, *85*, 1855–1864. [\[CrossRef\]](#)
44. Rowe, K.J.; Rutter, E.H. Paleostress estimation using calcite twinning: Experimental calibration and application to nature. *J. Struct. Geol.* **1990**, *12*, 1–17. [\[CrossRef\]](#)
45. Teufel, L.W. Strain analysis of experimental superposed deformation using calcite twin lamellae. *Tectonophysics* **1980**, *65*, 291–309. [\[CrossRef\]](#)
46. Evans, M.A.; Groshong, R.H. A Computer Program for the Calcite Strain-Gage Technique. *J. Struct. Geol.* **1994**, *16*, 277–281. [\[CrossRef\]](#)
47. Ferrill, D.A.; Morris, A.P.; Evans, M.A.; Burkhard, M.; Groshong, R.H.; Onasch, C.M. Calcite Twin Morphology: A Low-Temperature Deformation Geothermometer. *J. Struct. Geol.* **2004**, *26*, 1521–1529. [\[CrossRef\]](#)
48. Gray, M.B.; Stamatakos, J.A.; Ferrill, D.A.; Evans, M.A. Fault-Zone Deformation in Welded Tuffs at Yucca Mountain, Nevada, USA. *J. Struct. Geol.* **2005**, *27*, 1873–1891. [\[CrossRef\]](#)
49. Liu, J.; Davis, G.A.; Lin, Z.; Wu, F. The Liaonan Metamorphic Core Complex, Southeastern Liaoning Province, North China: A Likely Contributor to Cretaceous Rotation of Eastern Liaoning, Korea and Contiguous Areas. *Tectonophysics* **2005**, *407*, 65–80. [\[CrossRef\]](#)
50. Yang, T.N.; Peng, Y.; Leech, M.L.; Lin, H.Y. Fold patterns indicating Triassic constrictional deformation on the Liaodong peninsula, eastern China, and tectonic implications. *J. Asian Earth Sci.* **2011**, *40*, 72–83. [\[CrossRef\]](#)
51. Wang, Z.X.; Tang, Z.M.; Yang, Z.Z.; Yang, X.B. Redetermination of the Meso-Cenozoic structural framework of Dalian area. *Reg. Geol. China* **2000**, *19*, 120–126.
52. Avdeivitch, N.N. Geodynamic Evolution of the Cretaceous Liaonan Metamorphic Core Complex, Northeast China: New Insights from Calcite Twin Paleostress Analysis. Honors Thesis, Macalester College, St. Paul, MN, USA, 2013; p. 63.
53. Nuriel, P.; Weinberger, R.; Kylander-Clark, A.R.C.; Hacker, B.C.; Craddock, J.P. The onset of the Dead Sea transform based on calcite age-strain analyses. *Geology* **2017**, *45*, 587–590. [\[CrossRef\]](#)
54. Conel, J.E. Studies of the Development of Fabrics of Some Naturally Deformed Limestones. Ph.D. Thesis, California Institute of Technology, Pasadena, CA, USA, 1962; p. 257.
55. Fletcher, R.C. Analysis of flow in layer viscous fluids at small, but finite amplitude, with application to mullion structures. *Tectonophysics* **1982**, *81*, 51–66. [\[CrossRef\]](#)
56. van der Pluijm, B.A.; Craddock, J.P.; Graham, B.R.; Harris, J.H. Paleostress in Cratonic North America; Implications for Deformation of Continental Interiors. *Science* **1997**, *277*, 794–796. [\[CrossRef\]](#)
57. Craddock, J.P.; van der Pluijm, B.A. Regional stress-strain fields of Sevier-Laramide tectonism from calcite twinning data, west-central North America. *Tectonophysics* **1999**, *305*, 275–286. [\[CrossRef\]](#)
58. Craddock, J.P.; Jackson, M.; van der Pluijm, B.A.; Versical, R. Regional shortening fabrics in eastern North America: Far-field stress transmission from the Appalachian–Ouachita orogenic belt. *Tectonics* **1993**, *12*, 257–264. [\[CrossRef\]](#)
59. Craddock, J.P.; Malone, D.H.; Porter, R.; Luczaj, J.; Konstantinou, A.; Day, J.E.; Johnston, S.T. Paleozoic reactivation structures in the Appalachian–Ouachita–Marathon foreland: Far-field deformation across Pangea. *Earth-Sci. Rev.* **2017**, *169*, 1–34. [\[CrossRef\]](#)
60. Craddock, J.P. Transpression during tectonic evolution of the Idaho-Wyoming fold-and-thrust belt. *Geol. Soc. Am. Mem.* **1992**, *179*, 125–139.



61. Craddock, J.P.; Craddock, S.D.; Konstantinou, A.; Kylander-Clark, A.; Malone, D.H. Calcite Twinning Strain Variations across the Proterozoic Grenville Orogen and Keweenaw-Kapuskasing Inverted Foreland, USA and Canada. *Geosci. Front.* **2017**, *8*, 1–29. [[CrossRef](#)]
62. Klein, T.; Craddock, J.P.; Zulauf, G. Constraints on the geodynamical evolution of Crete: Insights from illite crystallinity, Raman spectroscopy and calcite twinning above and below the “Cretan detachment”. *Int. J. Earth Sci.* **2013**, *102*, 139–182. [[CrossRef](#)]



© 2018 by the authors. Licensee MDPI, Basel, Switzerland. This article is an open access article distributed under the terms and conditions of the Creative Commons Attribution (CC BY) license (<http://creativecommons.org/licenses/by/4.0/>).